EXPERIMENTAL INVESTIGATION OF USING GRAPHENE NANOPLATELETS AND HYBRID NANOFLUID AS COOLANT IN PHOTOVOLTAIC THERMAL SYSTEMS

by

Omran ALSHIKHI[a*] and Muhammet KAYFECI[b]

[a] Department of Energy Systems Engineering, Institute of Graduate Studies, Karabuk University, Karabuk, Turkey
[b] Department of Energy Systems Engineering, Faculty of Technology, Karabuk University, Karabuk, Turkey

Original scientific paper
https://doi.org/10.2298/TSCI200524348A

It is a common observation that the photovoltaic (PV) panel shows a compromised performance when its temperature rises. To handle the performance reduction, most PV panels are equipped with a thermal absorber for removing the solar cells' excessive heat with the help of a heat transfer fluid. The mentioned thermal absorber system is termed as PV thermal or simply PV/T. This study aims to experimentally investigate the effects of a graphene nanoplatelets nanofluid, distilled water, and hybrid nanofluid as transfer fluids in PV/T collectors. A hybrid nanofluid comprises Al_2O_3 and graphene nanoplatelets. An outdoor experimental set-up was installed and tested under the climatic conditions in Karabuk, Turkey, to measure the inlet as well as outlet PV/T fluid temperatures, ambient temperature with solar radiation, and surface temperatures of both PV/T collector and the PV panel. The mass percentage of the coolant fluids was 0.5% (by weight) and their flow rate was 0.5 Lpm. Results show that the graphene nanoplatelets nanofluid is the most effective fluid because it showed superior thermal efficiency among all the tested fluids. Adding a thermal unit to the PV/T unit increased the overall energy efficiency by 48.4%, 52%, and 56.1% using distilled water, hybrid nanofluid, and graphene nanofluid, respectively.

Key words: *photovoltaic thermal unit, energy performance, nanofluids, graphene nanofluid, hybrid nanofluid*

Introduction

Energy systems rely on fossil fuels all over the world, which dramatically decrease when their consumption increases, and it requires focus on producing alternative energy sources.The issue of GHG emerged as a consequence of fossil fuel combustion. According to estimates, the global energy demands are expected to increase further 45% until 2030 (1.6% annually) [1]. Now, most developed nations are attempting to switch to common renewable energies to generate power, including wind, solar, and biofuels. The solar energy is received and used through thermal systems for power generation through PV effect. Generally, just 5-20% of incident solar radiation, which is received using conventional PV modules, can actually be transformed into electricity while the leftover solar energy stores as heat in a PV [2]. Generally,

* Corresponding author, e-mail: oalshikhi@gmail.com

silicon solar cells are used to convert some radiation into electricity while the residual solar radiation converts into thermal power.

Normally, it is possible to convert 7% radiation into electricity when amorphous silicon is used while 16% radiation can be converted into electricity when cadmium telluride is used. Some radiation mediates and transforms into heat, which raises the cell temperature and diminishes both efficiency and output of a cell. Thermal collectors can collect this heat for heating water and air [3] using PV/T units rather than using just PV. It reduces the two separate systems' position areas, materials, and costs besides improving the overall efficiency. Typically, a PV cell's heat recovers when a cooling medium is applied that can be air, liquid, or a mix of both. The PV/T systems simultaneously generate both electric and thermal energies using the same surface area. Several researchers have used air [4], water [5-8] and nanofluids to cool down PV or reduce their surface temperatures by using a number of ways, including spraying water [9] and running a water film on the back surface of a PV with the help of nozzles [10]. Nanofluids are mixtures of phase-solid nanoparticles and de-ionized water, which are different as compared to conventional cooling fluids [11]. Nowadays, nanofluids have widespread applications and they have unique heat transfer characteristics, substantial thermal conductivity, and enhanced heat transfer mechanisms. Moreover, they have the ability to decrease the temperature in PV/T collectors and a number of devices. Nanofluids have two varieties. Single nanofluid that is made using a single type of nanoparticles and a hybrid nanofluid, which is a mix of various nanoparticles and base liquids. Bhattacharjee *et al*. [12] performed experimental investigations using three different designs of solar PV panel (circular spiral, circular spiral semi-flattened, and semi-oval serpentine) to absorb heat on the back surface. The results showed that a circular spiral semi-flattened absorber most optimally performed among all the investigated types because it showed highest efficiency (4.32%) and fill factor (19.80%). In a recent indoor study, Al-Waeli *et al*. [13] tested Al_2O_3, CuO, and SiC-based nanofluids for performance enhancement of PV/T systems at 4.0% concentration by volume. They attached a 110 W PV panel to a solar collector to construct their PV/T. They cooled their working fluid by-passing it through a storage tank. According to the results, SiC nanoparticles showed superior stability and thermal conductivity, which can improve the PV/T system performance as compared to the other two nanofluids. In another study, Al-Waeli *et al*. [14] used three different types of nanoparticles in water-based fluids with different volumes to determine the nanoparticles' best concentration, which is appropriate to cool down an indoor PV/T system. They selected CuO, SiC, and Al_2O_3, nanoparticles and added them to water by volume (0.5, 1, 2, 3, and 4%). Results showed that adding nanoparticles improves the thermal conductivity of the fluid that slightly increases the density and viscosity as compared to water. A suspension with SiC nanoparticles showed higher stability and thermal conductivity when it was compared to the suspensions with other nanoparticles. The fluid containing CuO had the next best thermal conductivity while Al_2O_3 showed the least thermal conductivity but the fluid's output stability was lower. The results showed stabilizing properties of the three selected materials.

In another study, Vakili *et al.* [15] conducted experiments on de-ionized water and graphene nanoplatelets (GNP) in a solar collector. Until then, GNP nanofluid was not used as a working fluid in any volumetric solar collector. Their results showed an ideal mass-flow rate (0.015 kg/s) with zero-loss efficiency while weight fractions at 0.0005, 0.001, and 0.005 were 83.50%, 89.70%, and 93.20%, respectively. It was 70% when a base fluid was used. Ebaid *et al*. [16] conducted experiments to investigate a couple of nanofluids and water as coolants at volumetric flow rate 0.5-5 Lpm (0.01 wt.%, 0.05 wt.%, and 0.1 wt.%). They used TiO_2 in a water-cetyl tri-methyl ammonium bromide mixture (pH 9.7), Al_2O_3 in a water-polyethylene glycol mixture (pH 5.7), and concluded that both types of nanofluid cooling substantially reduced the average PV cell temperature after comparing the results of using water as a coolant. They declared that the Al_2O_3 nanofluid outperformed as compared to the TiO_2 nanofluid while higher nanofluid concentrations produced a better cooling effect on the PV cell. Moreover, the electrical power and efficiency analyses revealed that the TiO_2 nanofluid performed better than water. Another experimental investigation by Iranmanesh *et al*. [17] analyzed the effect of using a graphene nanoplatelet distilled water nanofluid on the thermal performance of a tube solar collector water heater. The flow rates of 0.5, 1, and 2 Lpm were selected for different nanofluid concentrations (0.025 wt.%, 0.5 wt.%, 0.75 wt.%, and 0.1 wt.%). They reported that the mentioned nanofluid improved the thermal efficiency of the solar collector by up to 90.7% at 1.5 Lpm when it was used as an absorption medium. A mathematical model was proposed by Al-Waeli *et al*. [18] that discussed a new nanofluid/nano PCM PV/T system. This model was tested by conducting experiments using silicon carbide-water nanofluid and silicon carbide-PCM in the PV/T system. The comparison proved effectiveness of the proposed mathematical model. Sangeetha *et al*. [19] showed the effects outdoors of nanofluids (Al_2O_3, CuO, and MWCNT) mixed with water at 0 vol.%, 0.5 vol.%, 1 vol.%, 2.5 vol.%, and 5 vol.% on PV/T systems. They showed that MWCNT and CuO reduced cell temperatures by nearly 19%. The MWCNT, Al_2O_3, and CuO, respectively, produced electrical efficiency improvement by approximately 60%, 55%, and 52% greater than the conventional PV. Moreover, Al_2O_3, CuO, and MWCNT on PV/T systems produced a greater exergy efficiency than the conventional PV. Alous *et al*. [20] studied the performances of GNP mixed in water as a base fluid (flow rate: 0.5 Lpm, 0.5 wt.%) and PV/T systems of multi-walled carbon nanotubes. The MWCNT-water mixture performed better for PV energetic conversion as compared to graphene and distilled water. They reported that the graphene-water nanoplatelets have shown the highest thermal energetic efficiency. Furthermore, the total energy efficiency increased by 63.1% for graphene-water, 57.2% for MWCNT water, and 53.4% for distilled water. The total exergy efficiency increased by 12.1%, 20.6%, and 11.2% for the PV/T collector when it was cooled using MWCNT-water nanofluid, GNP water nanofluid, and distilled water, respectively.

Our study aims to divert the research community's attention wards using hybrid nanofluid (HyNF) as coolants in PV/T collectors, which is still rare in the literature. This study, to the best of our knowledge, is the first attempt to conduct experimental investigations on using a hybrid nanofluid of Al_2O_3 and GNP as a coolant in PV/T collectors. The hybrid nanofluid is made of two types of nanofluids (GNP and Al_2O_3), which has an equal quantity and concentration. Water and GNP were also used to achieve the same aim. The concentration for the coolants used were 0.5 wt.%, at coolants' flow rate 0.5 Lpm. Moreover, a PV/T collector is designed using a rectangular tube heat exchanger and a sheet. The experiment was designed, and both PV/T and PV were installed at the same level and direction, and they were exposed to the same factors. Also, all experiments have been conducted outdoor at the University of Karabuk, Turkey, at different experimental days. The analysis of the obtained results was conducted from energetic perspective and they were compared with water-cooled PV/T system and PV module results. The thermal and electrical energy efficiencies were calculated and compared with the other aforementioned research results.

Experimental set-up

An experimental test rig was constructed at the Karabuk University, Turkey, between August and October, 2019. It used a two 20 W polycrystalline PV module. One of them was used to construct a PV/T collector, which can be seen in fig. 1. The PV module specifica-

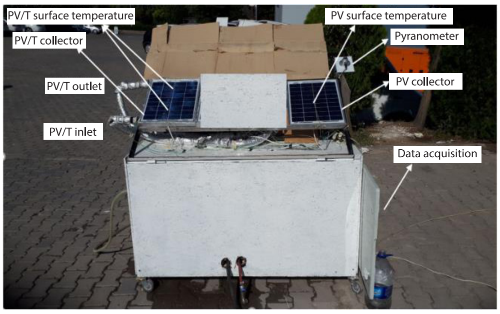

Figure 1. Picture of the experimental set-up

tions have been listed in tab. 1. A 1 mm thick copper plate was installed on the PV unit's bottom surface and soldered with a copper tube as a single unit. The tube was square in shape with 10 mm outer dimension and 8 mm inner dimension. Also, it was installed below the thermal barrier insulation maintain the effectiveness of heat exchange. Thermal paste was used to ensure the perfect contact between the copper plate and the surface behind the PV module.

Moreover, there were extra components in the system, which are shown in fig. 2. We used a Nova RS25/4G130 pump to run the fluids through the nanofluid storage tank, PV/T collector, and heat exchanger for cooling down the warm fluid. We used a Sea YFS201 flow meter for measuring and controlling the coolant flow rate at 0.5 Lpm. We connected the *K*-type thermocouples to a computer and eight channel data loggers (Pico, USB TC08 thermocouple data logger) for measuring the inlet and outlet fluid temperatures besides measuring ambient and surface temperatures.

Table 1. Specifications of typical PV/T panel

Model type	LXR-020P
Brand name	LEXRON
Electrical characteristics	
Rated maximum power, P_{max}	20 Wp
Power tolerance range	+5%
Open circuit voltage, V_{oc}	22.10 V
Maximum power voltage, V_{mp}	18.00 V
Short circuit current, I_{sc}	1.35 A
Maximum power current, I_{mp}	1.11A
Maximum system voltage	1000 V
Maximum sense fuse rating	10.0 A
Dimension	41.20 × 33.60 cm

Solar radiation was measured by using an EKO MS602 (Japan) pyranometer, which was connected to a data collecting board with a 4.2 inch screen Arduino and SD card. The PV/T collector and PV module were inclined at a constant 30° angle of inclination wards south and tested under identical conditions. All data were simultaneously collected every 12 seconds.

Testing procedure

We conducted numerous experiments in August, September, and October 2019 under consistent weather conditions, and noted the measurements. The experimental duration was 09:30-17:00 for tests pertaining to the GNP, distilled water, HyNF, and PV/T coolant inlet and outlet temperatures. We also measured solar irradiance, PV and PV/T surface temperatures, and generated current and voltage for PV and PV/T simultaneously every 12 seconds with a regular flow rate (0.5 Lpm) during the experiment. Then, the data collection during the selected days was used to compute averages and for further calculations. We also studied and compared theperformances of the PV/T water-cooled, PV/T nanofluid-cooled, and PV modules.

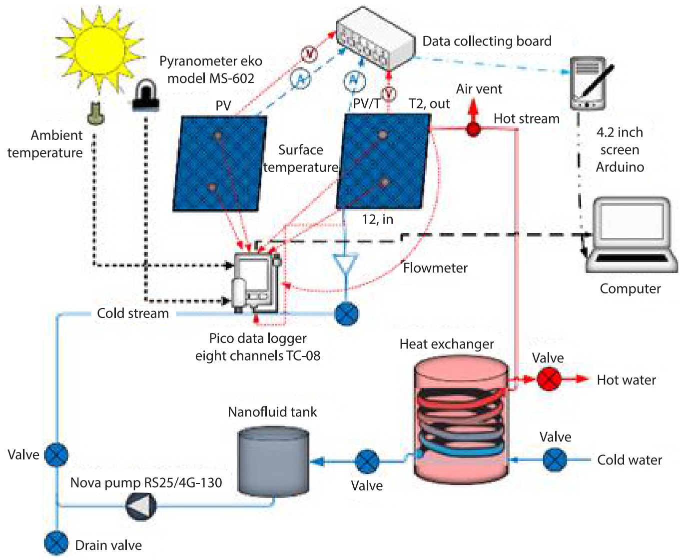

Figure 2. Schematic diagram of the experimental set-up

Preparation of nanofluids

The hydrous dispersion of the GNP (112 μm diameter, 0.551.2 nm thickness, more than 99.3 wt.% purity, and 5001200 m^2/g specific surface area), HyNF consisting of 1:1 0.5 GNP, 0.5 Al_2O_3 concentrations, and Al_2O_3 nanofluids with particle sizes of 3040 nm and 99.9% purity were obtained from NANOGRAFI Co. Ltd. in Turkey. Table 2 shows the thermal properties of both nanoparticles. Figure 3 shows SEM image of GNP and Al_2O_3 nanofluids. It could be observed that all the particles are almost sheet and spherical in shape figs. 3(a) and 3(b) and nanosized in the range of 10-30 nm with small agglomeration. Figure 4 shows the nanofluid samples after finishing the nanofluid preparation while sedimentation was not observed when experiments were conducted.

Table 3 shows thermophysical properties of nanofluids and water, which were taken from the [21] and the GNP nanofluid [22].

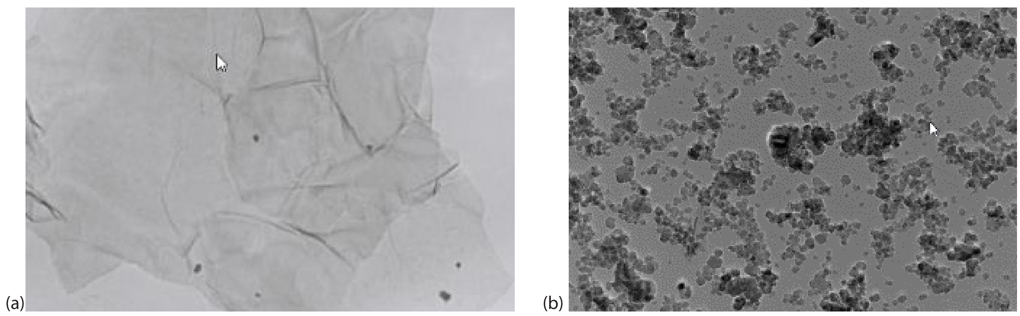

Figure 3. The SEM image of the nanoparticles; (a) GNP and (b) Al_2O_3

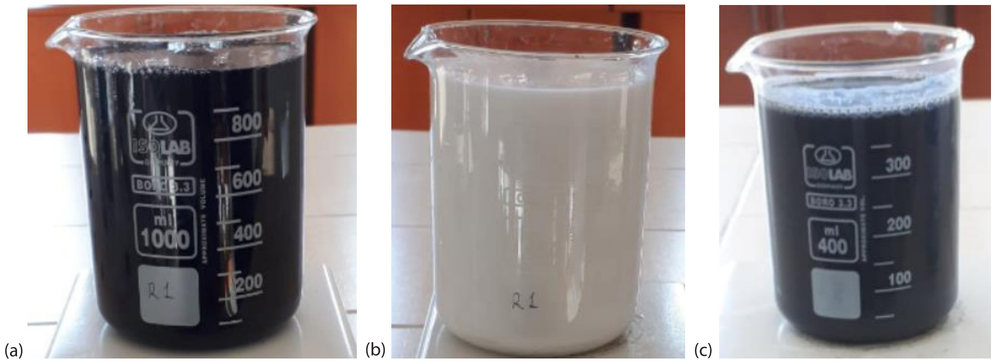

Figure 4. Samples of nanofluids; (a) GNP, (b) Al_2O_3, and (c) HyNF

Table 2. Thermophysical properties of water and nanoparticles [20, 21]

Property	Water	Al_2O_3	GNP
ρ [kgm^{-3}]	997.1	3970	2100
C_p [kJkg^{-1}K^{-1}]	4179	765	5000
k [Wm^{-1}K^{-1}]	0.613	40	0.710

Analysis

The density of nanofluids is obtained from [23]:

$$\rho_{\mathrm{nf}} = \varphi\rho_{\mathrm{np}} + (1-\varphi)\rho_{\mathrm{bf}} \tag{1}$$

where ρ_{bf} is the base fluid density, φ – the volume concentrations of the dispersed fluid, and ρ_{np} – the nanoparticles' density, otherwise, the density of the hybrid nanofluid is obtained [24]:

$$\rho_{\mathrm{h,nf}} = \varphi_{\mathrm{np1}}\rho_{\mathrm{np1}} + \varphi_{\mathrm{np2}}\rho_{\mathrm{np2}} + (1-\varphi_{\mathrm{tot}})\rho_{\mathrm{bf}} \tag{2}$$

The volume fraction of nanofluid can be calculated [25]:

$$\varphi = \frac{\dfrac{\dot{m}_{\mathrm{p}}}{\rho_{\mathrm{p}}}}{\dfrac{\dot{m}_{\mathrm{p}}}{\rho_{\mathrm{p}}} + \dfrac{\dot{m}_{\mathrm{f}}}{\rho_{\mathrm{f}}}} \tag{3}$$

where φ is the volumetric ratio of nanoparticles in a base fluid and ρ [kgm^{-3}] – the density. We used the following formula to calculate the volume fraction of a hybrid nanofluid [26]:

$$\varphi = \left[\frac{\left(\dfrac{\dot{m}}{\rho}\right)_{\mathrm{Al_2O_3}} + \left(\dfrac{\dot{m}}{\rho}\right)_{\mathrm{GNP}}}{\left(\dfrac{\dot{m}}{\rho}\right)_{\mathrm{Al_2O_3}} + \left(\dfrac{\dot{m}}{\rho}\right)_{\mathrm{GNP}} + \left(\dfrac{\dot{m}}{\rho}\right)_{\mathrm{EG}}}\right] \tag{4}$$

The following equation is used to obtain the heat capacity of nanofluids [5]:

$$\left(\rho C_p\right)_{\mathrm{nf}} = (1-\varphi)\left(\rho C_p\right)_{\mathrm{bf}} + \left(\rho C_p\right)_{\mathrm{p}} \tag{5}$$

where ρ [kgm^{-3}] is the denotesthe density, C_p [kJkg^{-1}K^{-1}] – the specific heat, and φ – the shows the volumetric ratio of nanoparticles in a base fluid. The subscripts bf, np, and nf are spectively represent base fluid, nanoparticles, and nanofluid. The heat capacity of HyNF is obtained [24]:

$$C_{p,\text{hnf}} = \frac{\varphi_{\text{np1}}\rho_{\text{np1}}C_{p,\text{np1}} + \varphi_{\text{np2}}\rho_{\text{np2}}C_{p,\text{np2}} + \left(1-\varphi_{\text{tot}}\right)\rho_{\text{bf}}C_{p,\text{bf}}}{\rho_{\text{hnf}}} \tag{6}$$

Maxwell-Garnet [27] model is used to calculate the nanofluids' thermal conductivity:

$$k_{\text{nf}} = \frac{k_{\text{p}} + 2k_{\text{f}} + 2\varphi\left(k_{\text{p}} - k_{\text{f}}\right)}{k_{\text{p}} + 2k_{\text{f}} - \varphi\left(k_{\text{p}} - k_{\text{f}}\right)}k_{\text{f}} \tag{7}$$

Also, the thermal conductivity of HyNF was represented [24]:

$$k_{\text{h,nf}} = k_{\text{bf}}\left[\frac{\dfrac{\varphi_{\text{np1}}k_{\text{np1}} + \varphi_{\text{np2}}k_{\text{np2}}}{\varphi_{\text{tot}}} + 2k_{\text{bf}} + 2\left(\varphi_{\text{np1}}k_{\text{np1}} + \varphi_{\text{np2}}k_{\text{np2}}\right) - 2\varphi_{\text{tot}}k_{\text{bf}}}{\dfrac{\varphi_{\text{np1}}k_{\text{np1}} + \varphi_{\text{np2}}k_{\text{np2}}}{\varphi_{\text{tot}}} + 2k_{\text{bf}}\left(\varphi_{\text{np1}}k_{\text{np1}} + \varphi_{\text{np2}}k_{\text{np2}}\right) + \varphi_{\text{tot}}k_{\text{bf}}}\right] \tag{8}$$

where φ is the volumetric ratio of nanoparticles in a base fluid and k [Wm^{-1}K^{-1}] – the thermal conductivity.

For performance evaluation of a nanofluid-based PV/T collector, we obtained the thermal variable Q_u:

$$Q_u = \dot{m}C_p\left(T_{\text{o}} - T_{\text{i}}\right) \tag{9}$$

where $\dot{m}$ [kgs^{-1}] is the coolant mass-flow rate, T_{i} and T_{o} are coolant inlet and outlet temperatures, and C_p [kJkgs^{-1}K^{-1}] – the coolant specific heat.

The PV and PV/T model'selectrical power output is obtained:

$$P = I \times V \tag{10}$$

where V [V] is the output voltage and I [A] is the output current.

The PV/T collector extracts thermal efficiency from solar radiation. The electrical, η_{el}, and thermal, η_{th}, efficiencies are:

$$\eta_{\text{th}} = \frac{Q_u}{I_R \times A_{\text{PVT}}} \tag{11}$$

$$\eta_{\text{el}} = \frac{P}{I_R \times A_{\text{PV}}} \tag{12}$$

where A_{PV} and A_{PVT} [m^2] are the area of PV cells and PV/T collector and I_R [Wm^{-2}] – the shows the total incident solar radiation on the PV and PV/T surfaces.

The thermal and electrical efficiencies to assess the overall energetic efficiency of a PV/T collector, η_{ov}, is [28]:

$$\eta_{\text{ov}} = \eta_{\text{th}} + r\eta_{\text{el}} \tag{13}$$

where $r = A_{\text{PV}}/A_{\text{th}}$ is the packing factor.

The electrical efficiency increment Δ_{el}:

$$\Delta_{el} = \frac{\eta_{PV/T,el} - \eta_{PV,el}}{\eta_{PV,el}} \times 100\% \tag{14}$$

Table 3. Thermophysical properties of the studied nanofluids

Property	GNP	HyNF
ρ [kgm^{-3}]	1259.5	1315
C_p [kJkg^{-1}K^{-1}]	2803	2873
k [Wm^{-1}K^{-1}]	1.1755	1.0110

Thermophysical properties for the nanofluids are obtained by eqs. (1)-(8).

Results and discussion

For this study, several experiments were conducted on the cooling operations of PV/T modules. All the measurements were collected after every 12 seconds in fig. 5 from 09:30 a. m. to 17:00 p. m. at flow rate 0.5 Lpm and it is calculated for two time periods. The first was the all-day period from 09:30 a. m. to 17:00 p. m. and the second was the peak period from 11:15 a. m. to 15:15 p. m. for all the coolants under investigation. Firstly, the distilled water experiment was performed on August 27, 2019 at flow rate 0.5 Lpm under stable weather conditions.

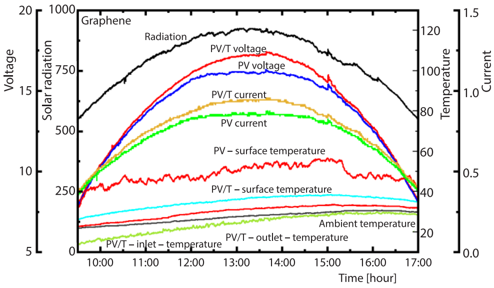

Figure 5. Parameters measured after every 12 seconds

Secondly, the same experiment was conducted for the GNP on September 18, 2019 at flow rate 0.5 Lpm. Finally, the experiment using HyNF was conducted on October 1, 2019 at flow rate 0.5 Lpm. Because of unstable weather conditions on other days, we ignored the results of several experiments of unstable results.

Solar irradiance and ambient temperature

The experimental module was tilted about 30° and directed towards south, which is an appropriate direction receive solar radiation. As we can see in fig. 6, the highest ambient temperature reached its peak at around 15:15 p. m. After which, it started to decrease to 30 °C by the end of the experiments at 17:00 p. m. Moreover, the solar radiation reached its peak at about 908 W/m^2 at 13:45 p. m., which gradually decreased to 530 W/m^2 by 17:00 p. m. All data taken from the experiments are presented in fig. 6.

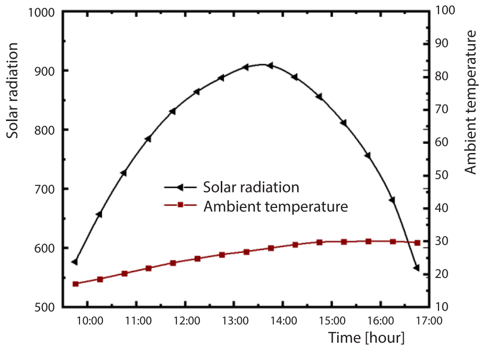

Figure 6. Ambient temperature on the experiment day and daily average solar radiation intensity

The surface temperature measurements

Figure 7 shows the PV/T and PV collectors' surface temperatures during the cooling times for both water and nanofluids from 09:30 a. m. to 17:00 p. m. The PV/T collector's surface temperature reduced more quickly when a coolant was used. The first experiment was conducted on August 27, 2019 from 09:30 a. m. to 17:00 p. m. and distilled water was used for cooling when the ambient temperature and solar radiation were high, and the daylight duration was longer. Moreover, at 09:30 a. m., the PV/T and PV surface temperatures were 30 °C and 46 °C, respectively, and reached a high temperature (38 °C) for the PV/T at 14:15 p. m. and 56 °C for the PV at 13:00 p. m. After the middle of the day, the radiation was lower, which decreased the PV surface temperature. However, the inlet, outlet, and PV/T surface temperatures were not affected due to the heat gained by the coolant and to insufficient time to respond and they progressively decreaseduntil the end of the test, which is shown in fig. 7(a).

The second experiment was conducted on September 18, 2019 from 09:30 a. m. to 17:00 p. m. using GNP fluid for cooling. As shown in fig. 7(b), the weather was steady most of the day and the surface temperatures for the PV/T and PV increased gradually from 27 °C and 39.5 °C at 09:30 a. m. to 38 °C and 54.8 °C at 14:45 p. m., respectively, which progressively decreased until 17:00 p. m. The third experiment was conducted on October 1, 2019 from 09:30 a. m. to 17:00 p. m. using HyNF for cooling. The solar radiation and ambient temperature were lower than the previous experiments and they were stable most of the test day fig. 7(c). The respective surface temperatures (PV/T and PV) were 26.8 °C and 39.8 °C at 9:30 a. m., which gradually increased to 37 °C and 52 °C, respectively, at 14:15 p. m. As a result, when the solar radiation increased, the PV and PV/T surface temperatures increased as well, and the coolant fluid temperatures also increased. The maximum surface temperature values for PV/T and PV collectors using distilled water, GNP, and HyNF were 14.2 °C, 14.4 °C, and 14 °C, respectively.

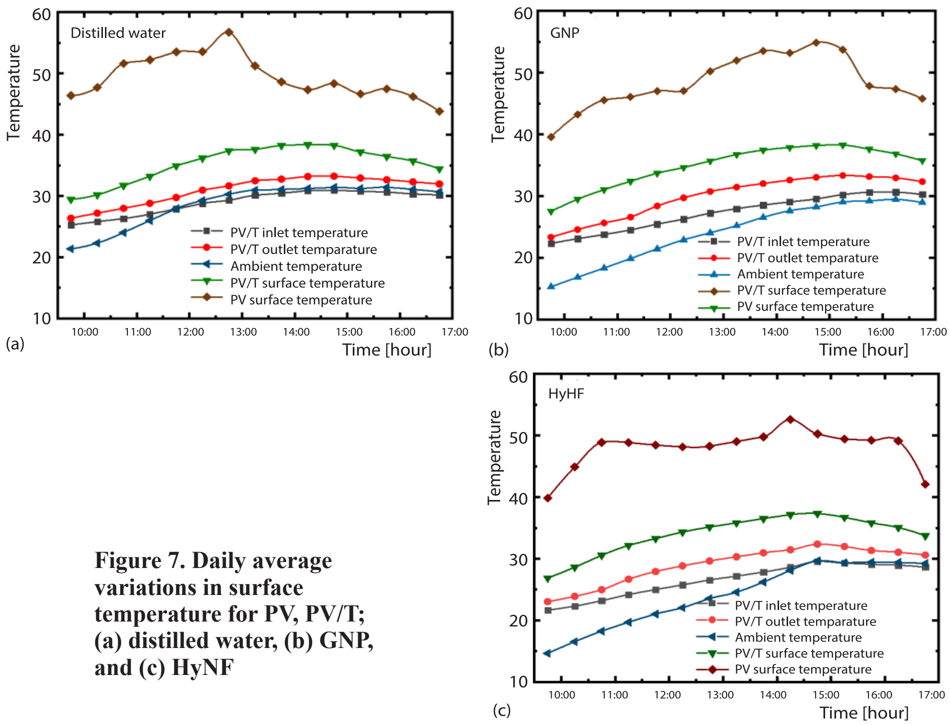

Figure 7. Daily average variations in surface temperature for PV, PV/T; (a) distilled water, (b) GNP, and (c) HyNF

Electrical efficiency and electrical power

As mentioned previously, we measured the surface temperature and its effect on the PV/T and PV surfaces and how to use the coolant to reduce the temperature to improve the electrical and the overall energy performance. Furthermore, the electrical energy and the power generated by the panels in relation PV and PV/T collectors always follow solar radiation, and it was noted that the maximum electric power was generated when the solar radiation was maximum. Tables 4 and 5 present the results of the solar radiation, electric efficiency of the PV and PV/T, surface temperature differences,and electrical efficiency increments for both time periods (all day and peak periods).

Table 4. The average daily weather conditions, electrical increment, andcell temperature during the day-long experiment

Type of coolant	I_R [Wm^{-2}]	T_{amb} [°C]	$T_{S,PV}$ [°C]	$T_{S,PV/T}$ [°C]	$\eta_{PV,el}$ [%]	$\eta_{PV/T,el}$ [%]	$\Delta_{ei,in}$ [%]
Water	803	28.4	49.4	35.2	8.8	9.6	8.7
Graphene	794	26.0	48.4	34.0	9.2	10.2	9.6
Hybrid	742	24.5	48.0	34.0	8.9	9.8	9.2

Table 5. Average daily weather conditions, electrical increment, and cell temperature during the peak period

Type of coolant	I_R [Wm^{-2}]	T_{amb} [C°]	$T_{S,PV}$ [C°]	$T_{S,PV/T}$ [C°]	$\eta_{PV,el}$ [%]	$\eta_{PV/T,el}$ [%]	$\Delta_{el,in}$ [%]
Water	893	29.6	51.0	37.0	10.2	11.4	10.5
Graphene	880	26.7	51.0	36.0	10.8	12.3	12.9
Hybrid	831	25.0	49.4	35.5	10.5	11.7	11.0

Figure 8 clearly indicates that the electrical power increases when solar intensity rises. However, during the experimental periods, the average daily solar radiation values using GNP nanofluid, HyNF, and distilled water were 803, 794, and 742 W/m^2, respectively. Moreover, all data taken from the experiments in terms of ambient temperature, radiation and electrical

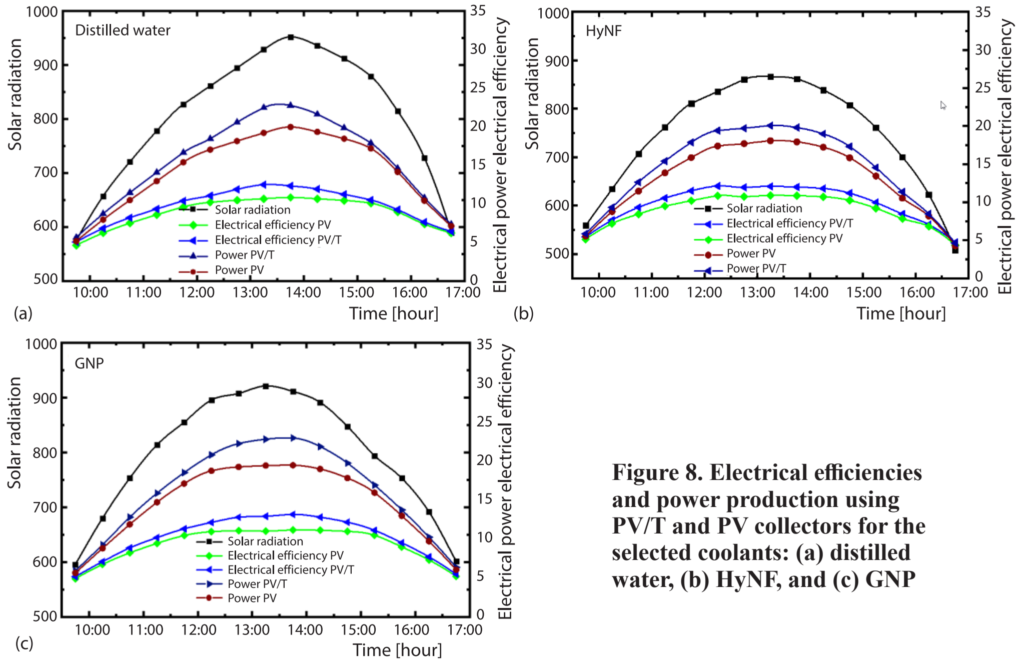

Figure 8. Electrical efficiencies and power production using PV/T and PV collectors for the selected coolants: (a) distilled water, (b) HyNF, and (c) GNP

efficiency increments were averaged and divided into two times, namely the day-long periods and peak periods, while we compared the performances of the coolants. Every coolant showed significant output electrical energy at 9.6%, 9.8%, and 10.2% for distilled water, HyNF, and GNP, respectively.

Electrical efficiency increment

As mentioned previously, the PV/T and PV surface temperatures increased when the solar radiation increased from the beginning to the end of the experiments, which decreased the electric efficiency of PV/T. In such cases, the heat is gradually extracted with the coolant fluid at a high temperature, which increases the electrical efficiency. As shown in fig. 9, GNP is the most electrically efficient fluid coolant as compared to rest of the coolants. This indicates that the GNP have higher thermal conductivity as compared to other coolants, which results in faster heat disposal, which is obtained by eq. (14). Tables 4 and 5 summarize the average daily electrical increments for the day-long and peak durations.

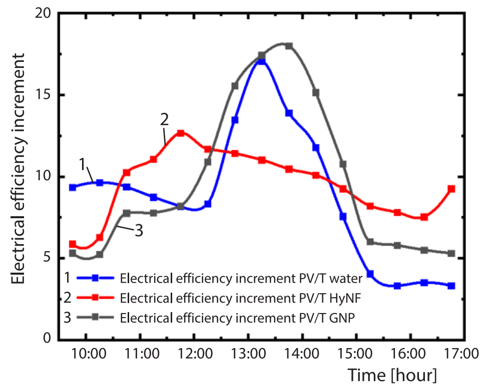

Figure 9. Daily average variation in electric efficiency

Thermal and overall energetic efficiency

In this study, the overall energy efficiency was calculated using eq. (13) as shown in fig. 10. Since the collector area covers all the PV cells and the collector while the PV cells have a perfect contact, the packing factor is equal to 1. The results showed that GNP are better than HyNF and distilled water because they have better thermal as well as overall energy efficiency. Moreover, the overall energy efficiency increased during the day when the thermal efficiency increased and the PV/T collector's energy extracted from solar energy is too close to the GNP and water values mentioned by Alous *et al*. [20] and distilled water values indicated by Sardarabadi *et al*. [29]. However, there are several factors, such as wind speed, change in solar radiation, and humidity, and all of them affect the thermal energy efficiency and make the thermal efficiency curve does not follow a specific trend as shown in fig. 11. As a result, the averages of the daily overall energy efficiency for the day-long periods were 48.1%, 53.5%, and 55.8% for distilled water, HyNF and GNP, respectively, and 50.1%, 58.9%, and 64.4%, respectively, for distilled wa-

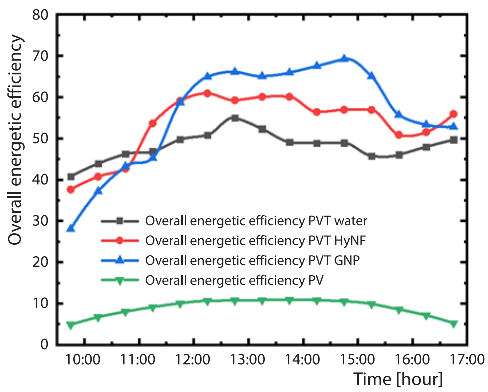

Figure 10. Average daily variation of PV and PV/T overall energetic efficiency

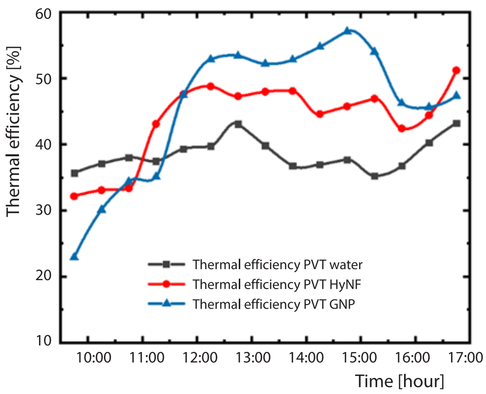

Figure 11. Average daily variation in thermal efficiencies for PV and PV/T

ter, HyNF and GNP during the peak period. The reference PV system showed 9.4% average overall efficiency when there was no collector (day-long period) and 10.7% for the peak period. This confirms that thermal cooling units should be used to improve the overall energy efficiency of a PV. We used eq. (11) to obtain the average daily thermal efficiency, which was 38.4% and 45.7% with PV/T for distilled water and GNP, respectively. These results are comparable to the values obtained in a study conducted by Alous *et al.* [20], who found respective values 38.8% and 47.4% for distilled water and GNP, which are compatible with the values given in tab. 6. The result for every experiment depended on different conditions such as ambient temperature, type of cooling, and intensity of solar radiation.

Table 6. Average daily thermal and overall energy efficiencies for PV/T with different coolants

Type of coolant	All day period		Peak period	
	η_{th} [%]	η_{ov} [%]	η_{th} [%]	η_{ov} [%]
Water	38.4	48.1	38.7	50.1
GNP	45.7	55.8	52.2	64.4
HyNF	43.7	53.5	47.3	58.9

Conclusions

In this study, the effects of GNP and HyNF as coolants were experimentally investigated for evaluating the thermal and electrical efficiencies of PV/T systems. The mentioned coolants include GNP, distilled water, and a HyNF (concentration: 0.5 wt.%, flow rate: 0.5 Lpm). The experiments were carried out when all the PV and PV/T had a tilt angle of nearly 30° to-compare a conventional PV system with a PV/T system. The results from this study revealed the following:

- Nanofluids and distilled water work as coolants through a cooling module, which reduces the maximum cell temperature for a PV/T system by approximately 14.2 °C, 14.4 °C, and 14 °C for distilled water, HyNF and GNP, respectively.
- The overall energy efficiency enhanced by 5.4% and 7.7% for the HyNF and GNP nanofluid as compared to the distilled water.
- The highest electrical energy generation level was observed when GNP nanofluid was used as a coolant.
- For a PV/T system, the thermal efficiency increased by nearly 5.3% and 7.3% more than the distilled water for HyNF and GNP nanofluids, respectively.
- The nanotechnology used in PV/T systems in the form of nanoparticles is more effective for hybrid system efficiency as a coolantas compared to distilled water.

Nomenclature

A_{PV} – PV surface area, [m²]
$A_{PV/T}$ – PV/T surface area, [m²]
C_p – heat capacity, [kJkg^{-1}K^{-1}]
I_R – solar radiation [Wm^{-2}]
k – thermal conductivity [Wm^{-1}K^{-1}]
$\dot{m}$ – mass-flow rate of a working fluid, [kgs^{-1}]
Q_u – thermal useful
r – packing factor of the PV cell
T_{amb} – ambient temperature, [°C]
$T_{S,PV}$ – PV surface temperature, [°C]
$T_{S,PV/T}$ – PV/T surface temperature, [°C]

Greek letters

$\Delta_{el,in}$ – electrical efficiency increment, [%]
η_{ov} – overall energetic efficiency, [%]
$\eta_{PV,el}$ – electrical efficiency PV, [%]
$\eta_{PV/T,el}$ – electrical efficiency PV/T, [%]
η_{th} – thermal efficiency, [%]
ρ – density, [kgm^{-3}]
φ – volume fraction

Subscript

bf – base fluid
f – fluid
p – particles
nf – nanofluid
np – nanoparticle

Acronyms

GNP – graphene nanoplatelets
HyNF – hybrid nanofluid

References

[1] Publishing, O., World Energy Outlook 2008, Organisation for Economic Co-operation and Development, Paris, France, 2008
[2] Abdallah, S. R., *et al.*, Experimental Investigation on the Effect of Using Nanofluid (Al_2O_3-water) on the Performance of PV/T system, *Thermal Science and Engineering Progress*, *7* (2018), Sept., pp. 1-7
[3] Al-Waeli, A. H., *et al.*, Modelling and Experimental Validation of a PV/T System Using Nanofluid Coolant and NanoPCM, *Solar Energy*, *177* (2019), Jan., pp. 178-191
[4] Mojumder, J. C., *et al.*, An Experimental Investigation on Performance Analysis of Air Type Photovoltaic Thermal Collector System Integrated with Cooling Fins Design, *Energy and Buildings*, *130* (2016), Oct., pp. 272-285
[5] Khanjari, Y., *et al.*, Numerical Investigation on Using of Nanofluid in a Water-Cooled Photovoltaic Thermal System, *Energy Conversion and Management*, *122* (2016), Aug., pp. 263-278
[6] Odeh, S. , Behnia, M., Improving Photovoltaic Module Efficiency Using Water Cooling, *Heat Transfer Engineering*, *30* (2009), 6, pp. 499-505
[7] Palaskar, V. N., Deshmukh, S., Performance Analysis of Especially Flow Design Heat Exchanger Used in Hybrid Solar System, *International Journal of Renewable Energy Research (IJRER)*, *5* (2015), 2, pp. 476-482
[8] Yazdanifard, F., *et al.*, Investigating the Performance of a Water-Based Photovoltaic/Thermal (PV/T) Collector in Laminar and Turbulent Flow Regime, *Renewable Energy*, *99* (2016), Dec., pp. 295-306
[9] Nižetić, S., *et al.*, Water Spray Cooling Technique Applied on a Photovoltaic Panel: The Performance Response, *Energy Conversion and Management*, *108* (2016), Jan., pp. 287-296
[10] Abdolzadeh, M., Ameri, M., Improving the Effectiveness of a Photovoltaic Water Pumping System by Spraying Water over the Front of Photovoltaic Cells, *Renewable Energy*, *34* (2009), 1, pp. 91-96
[11] Gao, Y., *et al*., Experimental Investigation of Specific Heat of Aqueous Graphene Oxide Al_2O_3 Hybrid nanofluid, *Thermal Science*, *25* (2019), 1B, pp. 515-525
[12] Bhattacharjee, S., *et al*., An Investigational Back Surface Cooling Approach with Different Designs of Heat-Absorbing Pipe for PV/T System, *International Journal of Energy Research*, *42* (2018), 5, pp. 1921-1933
[13] Al-Waeli, A. H., *et al*., Comparison Study of Indoor/Outdoor Experiments of a Photovoltaic Thermal PV/T System Containing SiC Nanofluid as a Coolant, *Energy*, *151* (2018), C, pp. 33-44
[14] Al-Waeli, A. H., *et al*., Comparative Study to Use Nano(Al_2O_3, CuO, and SiC) with Water to Enhance Photovoltaic Thermal PV/T Collectors, *Energy Conversion and Management*, *148* (2017), Sept., pp. 963-973
[15] Vakili, M., *et al*., Experimental Investigation of GNP Nanofluid-Based Volumetric Solar Collector for Domestic Hot Water Systems, *Solar Energy*, *131* (2016), June, pp. 119-130
[16] Ebaid, M. S., *et al*., Experimental Investigation of Cooling Photovoltaic (PV) Panels Using (TiO_2) Nanofluid in Water-Polyethylene Glycol Mixture and (Al_2O_3) Nanofluid in Water-Cetyltrimethylammonium Bromide Mixture, *Energy Conversion and Management*, *155* (2018), Jan., pp. 324-343
[17] Iranmanesh, S., *et al*., Thermal Performance Enhancement of an Evacuated Tube Solar Collector Using GNP Nanofluid, *Journal of Cleaner Production*, *162* (2017), Sept., pp. 121-129
[18] Al-Waeli, A.H., *et al*., Modelling and Experimental Validation of a PV/T System Using Nanofluid Coolant and Nano PCM, *177* (2019), Jan., pp. 178-191
[19] Sangeetha, M., *et al*., Progress of MWCNT, Al_2O_3, and CuO with Water in Enhancing the Photovoltaic Thermal System, *International Journal of Energy Research*, *44* (2019), 2, pp. 821-832
[20] Alous, S., *et al.*, Experimental Investigations of Using MWCNTs and GNP Water-Based Nanofluids as Coolants in PV/T Systems, *Applied Thermal Engineering*, *162* (2019), 114265
[21] Jia, Y., *et al*., Numerical Analysis of Photovoltaic-Thermal Collector Using Nanofluid as a Coolant, *Solar Energy*, *196* (2020), 11, pp. 625-636
[22] Contreras, E. M. C., *et al*., Experimental Analysis of the Thermohydraulic Performance of Graphene and Silver Nanofluids in Automotive Cooling Systems, *International Journal of Heat and Mass Transfer*, *132* (2019), Apr., pp. 375-387

[23] Pak, B. C., Cho, Y. I., Hydrodynamic and Heat Transfer Study of Dispersed Fluids with Submicron Metallic Oxide Particles, *Experimental Heat Transfer an International Journal*, *11* (1998), 2, pp. 151-170
[24] Al-Oran, O., *et al*., Exergy and Energy Amelioration for Parabolic trough Collector Using Mono and HyNF, *Journal of Thermal Analysis and Calorimetry*, *140* (2020), pp. 1579-1596
[25] Xuan, Y., Roetzel, W., Conceptions for Heat Transfer Correlation of Nanofluids, *International Journal of Heat and Mass Transfer*, *43* (2000), 19, pp. 3701-3707
[26] Nadooshan, A. A., *et al*., Measuring the Viscosity of Fe_3O_4-MWCNTs/EG Hybrid Nanofluid for Evaluation of Thermal Efficiency: Newtonian and non-Newtonian Behavior, *Journal of Molecular Liquid*s, *253* (2018), Mar., pp. 169-177
[27] Maxwell-Garnett, J. C., Colors in Metal Glasses and in Metallic Films, *Fill. Trans*, *203* (1904), pp. 385-420
[28] Chow, T. T., *et al*., Energy and Exergy Analysis of Photovoltaic-Thermal Collector with and Without Glass Cover, *Applied Energy*, *86* (2009), 3, pp. 310-316
[29] Sardarabadi, M., *et al*., Experimental Investigation of the Effects of Silica/Water Nanofluid on PV/T (Photovoltaic Thermal Units), *Energy*, *66* (2014), Mar., pp. 264-272

Paper submitted: May 24, 2020
Paper revised: November 12, 2020
Paper accepted: December 2, 2020